11th International Conference on Vibration Problems
Z. Dimitrovová *et.al.* (eds.)
Lisbon, Portugal, 9–12 September 2013

DAMAGE LOCALISATION IN BEAMS USING MIXED FINITE ELEMENTS

Pablo Moreno-García *[1], José V. Araújo dos Santos[2], Hernani M. R. Lopes [3]

[1]INEGI, Instituto de Engenharia Mecânica e Gestão Industrial,
Campus da FEUP, Rua Dr. Roberto Frias, 400,
4200-465 Porto, Portugal
pmorenogarcia@inegi.up.pt

[2]IDMEC, Instituto Superior Técnico,
Av. Rovisco Pais, 1049-001 Lisboa, Portugal
viriato@ist.utl.pt

[3]ESTIG, Instituto Politécnico de Bragança,
Campus de Sta. Apolónia, Apartado 134,
5301-857 Bragança, Portugal
hlopes@ipb.pt

Keywords: Damage Localisation, Mixed Finite Elements, Finite Differences, Modal Analysis, Curvatures.

Abstract. *Damage localisation is a very hot topic due to the important role that it assumes in preventing failures or breakdowns. In particular for beams, the method of mode shapes curvatures (second spatial derivative) is the most used method to achieve this goal. The usual way to compute these derivatives is the application of finite differences. These finite differences are usually applied to a mesh of finite elements, used as a reference (undamaged) model or in order to simulate the damage in the beams. However, there are several well-known problems in the use of finite differences, such as: the propagation and amplification of numerical errors. On the other hand, the mixed finite element method is a computational technique that provides the values of the bending moment, which is directly related with the curvature. In this work, a comparison between the quality of the damage localisation based on curvatures obtained using mixed finite elements and classical finite elements through the use of finite differences is presented. For the computation of the finite differences, an optimized sampling technique is proposed in order to reduce the noise propagation. Quality evaluators defined by the authors in a previous work are used to measure the quality of the damage localisation.*

1 INTRODUCTION

Damage localisation is a very hot topic due to the important role that it assumes in preventing failures or breakdowns of structures. Several methods based on vibration characteristics have been proposed over the years with this objective in mind [1–3]. A method based on the differences of mode shape curvatures of undamaged and damaged beams was proposed by Pandey et al. [4] and it is considered to be very efficient. The computation of curvatures in this work and subsequent ones (e.g. [5–8]) relies on the second order central finite difference formula. However, the application of these kind of formulas may lead to incorrect damage localizations, due to its intrinsic numerical errors. Furthermore, by applying the numerical differentiation to noisy data, the measurement errors are propagated and amplified, thus decreasing the quality of the damage localization. Also, due to the discontinuities at the boundary, the application of this method usually leads to high values of the differences of curvatures at the extremities of the beam [9, 10].

In order to minimize some of these problems, an improved method for damage localization using curvatures of the mode shapes is presented in this paper. This method relies on the computation of curvatures using the mixed finite element method. Mixed finite elements are based on mixed variational principles, where the secondary variables of the conventional principles are also treated as dependent variables [11]. The beam mixed finite element presented provides the values of the bending moment, which is directly related with the curvature. Thus, one can avoid the application of finite differences to the displacement field which is necessary when classical finite elements are used. A simply supported beam, subjected to damage at the midspan, is analyzed in order to illustrate the efficiency of the proposed approach to the damage localization using mixed finite elements and differences in curvatures.

2 FORMULATION

This Section presents the formulation of the mixed finite element used in this work, the definition of curvatures based on this finite element and the classical (displacement based) finite element. It also contains a description of an optimized sampling technique that is used to reduce the numerical noise propagation.

2.1 Mixed finite element

The governing equations of a Euler-Bernoulli beam can be written as [11]:

$$-\frac{d^2 M}{dx^2} - q = 0 \tag{1}$$

$$-\frac{d^2 w}{dx^2} - \frac{M}{EI} = 0 \tag{2}$$

where w is the transverse displacement, M is the bending moment, q is the distributed load, and EI is the bending stiffness of the beam. These equations are the foundations for the formulation of mixed finite elements to analyze Euler-Bernoulli beams. The formulation presented here is based on weak forms of Eqs. (1) and (2), but a weighted-residual method can also be used. A weak form over an element $\Omega^e = (x_a, x_b)$ is the following [11]:

$$0 = \int_{x_a}^{x_b} \left(\frac{dM}{dx}\frac{d\delta w}{dx} - q\delta w \right) dx + V_2\delta w\Big|_{x=x_b} - V_1\delta w\Big|_{x=x_a} \tag{3}$$

$$0 = \int_{x_a}^{x_b} \left(\frac{dw}{dx}\frac{d\delta M}{dx} - \frac{M}{E_e I_e}\delta M \right) dx + \theta_2\delta M\Big|_{x=x_b} - \theta_1\delta M\Big|_{x=x_a} \tag{4}$$

2

where δw and δM are, respectively, the virtual displacement and the virtual bending moment. The bending stiffness of the element is defined by $E_e I_e$. One sees that the transverse displacement w and the bending moment M are primary variables, while the rotation $\theta = dw/dx$ and the transverse force $V = dM/dx$, appearing in the boundary expressions, are secondary variables (see Figure 1).
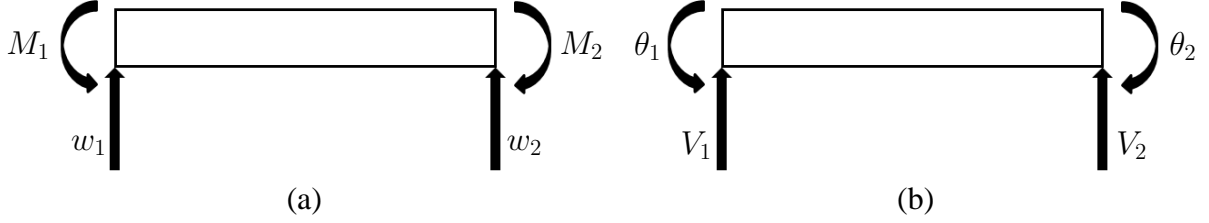

Figure 1: Type of variables of a beam mixed element: (a) two displacements and two bending moments as primary variables, and (b) two transverse forces and two rotations as secondary variables.

Since only first derivatives appear in the Eqs. (3) and (4), both the transverse displacement w and the bending moment M can be approximated using Lagrange interpolation:

$$w(x) \approx \sum_{i=1}^{m} w_i \phi_i(x), \quad M(x) \approx \sum_{i=1}^{n} M_i \psi_i(x), \tag{5}$$

where $\phi_i(x)$ and $\psi_i(x)$ are Lagrange interpolation functions. Substituting $w(x)$ and $M(x)$ in Eqs. (3) and (4), $\delta w = \phi_i$, $\delta M = \psi_i$, we obtain [11]:

$$\begin{pmatrix} [0] & [^{\phi\psi}A^e] \\ [^{\phi\psi}A^e]^T & -[^{\psi\psi}A^e] \end{pmatrix} \begin{pmatrix} \{w^e\} \\ \{M^e\} \end{pmatrix} = \begin{pmatrix} \{f^e\} + \{V^e\} \\ \{\bar{\theta}^e\} \end{pmatrix} \tag{6}$$

where

$$^{\phi\psi}A_{ij}^e = \int_{x_a}^{x_b} \frac{d\phi_i}{dx}\frac{d\psi_j}{dx}dx, \quad ^{\psi\psi}A_{ij}^e = \frac{1}{E_e I_e}\int_{x_a}^{x_b} \psi_i\psi_j dx, \tag{7}$$

$$f_i^e = \int_{x_a}^{x_b} q\phi_i dx, \quad \bar{\theta}_i^e = (-1)^{i+1}\theta_i^e \tag{8}$$

In dynamic analysis of beams a term related to the kinetic energy of the element with mass density ρ_e and cross section area A_e should be added to the equations that define the weak form:

$$K_e = \frac{1}{2}\int_{x_a}^{x_b} \rho_e A_e \left(\frac{dw}{dt}\right)^2 dx \tag{9}$$

This term is only function of the transverse displacement, yielding, in case of free vibrations, the matrix:

$$B_{ij}^e = \int_{x_a}^{x_b} \rho_e A_e \phi_i \phi_j dx \tag{10}$$

The matrices of all the elements need to be assembled as usual in order to obtain the global matrices and the generalized eigenvalue problem:

$$\begin{pmatrix} [0] & [^{\phi\psi}A] \\ [^{\phi\psi}A]^T & -[^{\psi\psi}A] \end{pmatrix} \begin{pmatrix} \{w\} \\ \{M\} \end{pmatrix} = \omega^2 \begin{pmatrix} [B] & [0] \\ [0] & [0] \end{pmatrix} \begin{pmatrix} \{w\} \\ \{M\} \end{pmatrix} \tag{11}$$

3

where the vectors $\{w\}$ and $\{M\}$ define, respectively, the mode shapes and the corresponding bending moments, and ω are the circular frequencies. The essential boundary conditions for the present mixed finite element are defined by:

$$w = \hat{w} \quad \text{on} \quad \partial\Omega_w \quad \text{and} \quad M = \hat{M} \quad \text{on} \quad \partial\Omega_M \tag{12}$$

while the natural boundary conditions are

$$V = \hat{V} \quad \text{on} \quad \partial\Omega_V \quad \text{and} \quad dw/dx = \hat{\theta} \quad \text{on} \quad \partial\Omega_\theta \tag{13}$$

These conditions are imposed by deleting the rows and columns of the global matrices corresponding to the constrained nodal degrees of freedom. The matrices thus obtained are condensed, yielding the reduced generalized eigenvalue problem

$$\left[\bar{A}\right]\left\{\bar{w}\right\} = \omega^2\left[\bar{B}\right]\left\{\bar{w}\right\} \tag{14}$$

where

$$\left[\bar{A}\right] = \left[{}^{\phi\psi}\bar{A}\right]\left[{}^{\psi\psi}\bar{A}\right]^{-1}\left[{}^{\phi\psi}\bar{A}\right]^{T} \tag{15}$$

and the bar denotes the global matrices after eliminating the rows and columns and the unconstrained transverse displacements. The unconstrained bending moments are computed by:

$$\left\{\bar{M}\right\} = \left[{}^{\psi\psi}\bar{A}\right]^{-1}\left[{}^{\phi\psi}\bar{A}\right]^{T}\left\{\bar{w}\right\} \tag{16}$$

In the present work, the Lagrange interpolation functions are linear for both the transverse displacement and the bending moment ($n = m = 1$ in Eq. (5)).

2.2 Damage localisation

In view of damage mechanics (see [12]), a parameter d_e can be defined such that the Young's modulus of an element e is given by:

$$\widetilde{E}_e = E_e(1 - d_e) \quad \text{with} \quad 0 \le d_e \le 1 \tag{17}$$

If $d_e = 0$ there is no reduction in the Young's modulus and, therefore on the bending stiffness, whereas if $d_e = 1$ there will be a complete reduction of stiffness. If one uses mixed finite elements, the curvature of a point with coordinate x_j in a damage beam is computed by:

$$\frac{d^2\widetilde{w}_{q,M}(x_j)}{dx^2} = -\frac{\widetilde{M}_q(x_j)}{\widetilde{E}_e I_e} \tag{18}$$

where the subscript q denotes the mode shape number, and the subscript M indicates that the computation is based on mixed finite elements. However, if one uses displacement based finite elements, the curvature needs to be computed using finite differences, since the bending moment is not available. Computing the second derivative with a four point formula, the curvature is approximated by:

$$\frac{d^2\widetilde{w}_{q,w}(x_j)}{dx^2} \approx \frac{1}{3h_x^2}\sum_{i=0}^{3} P_i\widetilde{w}_{q,w}(x_i) \tag{19}$$

where the subscript w indicates that the transverse displacements are computed using conventional finite elements. The coefficients P_i are presented in References [13–15].

4

If the beam is not damaged, the curvature in any point is computed analytically using results coming from the application of the Ritz method:

$$\frac{d^p w_q(x_j)}{dx^p} = \sum_{n=1}^{N} W_n \frac{d^p X_n(x_j)}{dx^p} \tag{20}$$

where p is the order of the derivative ($p = 2$ for curvatures), W_n are coefficients obtained by solving an eigenvalue problem and $X_n(x)$ are analytical functions defined by Gartner and Olgac [16]. This problem is detailed for plates in [14, 15].

Once the curvatures are computed and normalized in the same way, by setting the absolute maximum value equal to one, the following damage indicators are used:

$$CD_{q,w}(x_j) = \left| \frac{d^2 \widetilde{w}_{q,w}(x_j)}{dx^2} - \frac{d^2 w_q(x_j)}{dx^2} \right| \tag{21}$$

$$CD_{q,M}(x_j) = \left| \frac{d^2 \widetilde{w}_{q,M}(x_j)}{dx^2} - \frac{d^2 w_q(x_j)}{dx^2} \right| \tag{22}$$

These indicators correspond to $DFD_q^p(x,y)$ in References [14, 15] for one-dimensional case, being $p = 2$. Also, quality evaluators similar to the ones defined in [15] are used:

$$\mu_{q,w} = 1 - \frac{\sum_{k=1}^{NN} (\overline{CD}_{q,w})}{NN}, \text{ with } \overline{CD}_{q,w} \leq 1 \tag{23}$$

$$\mu_{q,M} = 1 - \frac{\sum_{k=1}^{NN} (\overline{CD}_{q,M})}{NN}, \text{ with } \overline{CD}_{q,M} \leq 1 \tag{24}$$

where NN is the number of nodes and the overline denotes that the damage indicators are normalised such that the maximum value is equal to one.

2.3 Optimum sampling

The method to obtain the optimum sampling in order to minimize the influence of the noise is briefly explained here for the one-dimensional case (beams) and second derivative, and more details can be obtained in Reference [17]. Due to the finite difference method itself, there is an error which depends on the order of the derivative p, the number of points used, the point where the derivative is computed, the sampling h_x, and the values of a higher order derivative of the mode shape $\widetilde{w}_q(\zeta)$, $\zeta \in [x_0, x_m]$. This error will be called error of the method and denoted by $\check{E}_q^{(m)}$. Besides this error, there are other type of errors associated with the numerical computations. This error will be denoted by $\check{E}_q^{(r)}$, and depends on the relative numerical accuracy ϵ, the sampling h_x, the coefficients P_i and the values of the mode shape $\check{w}_q(\zeta)$, $\zeta \in [x_0, x_m]$. The coefficients P_i are defined by the order of the derivative p, the number of points used and the point where the derivative is computed.

Assuming that the mode shape contains round-off errors, the real (damaged) mode shape value $\widetilde{w}_q(x_j)$ is:

$$\widetilde{w}_q(x_j) = \check{w}_q(x_j) \pm \check{E}_q(x_j) \tag{25}$$

where $\check{w}_q(x_j)$ represents a numerical value and $\check{E}_q(x_j)$ represents the round-off error. This round-off error is such that the following inequalities hold:

$$\check{E}_q(x_j) \leq \check{w}_q(x_j)\frac{\epsilon}{2} \leq \max|\check{w}_q(x_j)|\frac{\epsilon}{2}, \ x_j \in [0, L] \tag{26}$$

being L the length of the beam.

In this work, the second derivative of the mode shapes was computed using finite differences with four points (see Eq. (19)). The optimum sampling is computing with the finite difference formula of the interior points. In this case, the formula agrees with the central finite difference using three points (see [13]):

$$\frac{d^2\widetilde{w}_q(x_j)}{dx^2} = \frac{\widetilde{w}_q(x_{j-1}) - 2\widetilde{w}_q(x_j) + \widetilde{w}_q(x_{j+1})}{h_x^2} \pm \check{E}_q^{(m)}(x_j) \tag{27}$$

where

$$\check{E}_q^{(m)}(x_j) \leq \frac{h_x^2}{12}\max\left|\frac{d^4\widetilde{w}_q(\zeta)}{dx^4}\right| \tag{28}$$

According to this inequality, in order to compute the maximum error associated with the method $\check{E}_q^{(m)}$, it is necessary to know the values of the fourth derivative of the damaged mode shape, which, in general, is not possible. However, this difficulty can be overcomed by using the Ritz method. Because this method allow us to analytically compute the derivatives of any order, we can approximate the maximum of the fourth derivative of the mode shape by the maximum of the corresponding fourth derivative of the undamaged Ritz mode. This is accomplished by considering Eq. (20) with $p = 4$:

$$\max\left|\frac{d^4\widetilde{w}_q(\zeta)}{dx^4}\right| \simeq \max\left|\frac{d^4 w_q(\zeta)}{dx^4}\right| \leq \max\left|\frac{d^4 w_q(x)}{dx^4}\right|, \ x \in [0, L] \tag{29}$$

On the other hand, considering Eq. (25):

$$\frac{d^2\widetilde{w}_q(x_j)}{dx^2} = \frac{\check{w}_q(x_{j-1}) - 2\check{w}_q(x_j) + \check{w}_q(x_{j+1})}{h_x^2} + \check{E}_q^{(r)}(x_j) + \check{E}_q^{(m)}(x_j) \tag{30}$$

where, attending to Eq. (26),

$$\check{E}_q^{(r)}(x_j) \leq \frac{2\epsilon}{h_x^2}\max|\check{w}_q(\zeta)| \leq \frac{2\epsilon}{h_x^2}\max|\check{w}_q(x)|, \ x \in [0, L] \tag{31}$$

Therefore, the total error is given by:

$$\check{E}_q^{(t)}(x_j) = \check{E}_q^{(r)}(x_j) + \check{E}_q^{(m)}(x_j) \leq \frac{2\epsilon}{h_x^2}\max|\check{w}_q(x)| + \frac{h_x^2}{12}\max\left|\frac{d^4 w_q(x)}{dx^4}\right| = \check{E}_q^{(t,\max)}(x_j) \tag{32}$$

and the optimum sampling for each mode is computed as the one that minimizes the maximum total error:

$$\frac{d\check{E}_q^{(t,\max)}(x_j)}{dh_x} = 0 \tag{33}$$

3 RESULTS

A thin steel beam with a length of 1 m, a width of 0.01 m, and a thickness of 0.002 m is analyzed. The Young's modulus and the mass density are, respectively, 210 GPa and 7800 kg/m^3. The beam is discretized with four different meshes, corresponding to the optimum h_x for every one of its first four mode shapes, according to Section 2.3. These four mode shapes are computed with each one of the discretizations described in Table 1. All the computations presented in this work were performed using single precision. The boundary conditions are such that the beam is simply supported in both ends. Damage is applied in the element at the center of the beam by imposing three different values of d_e: 0.1, 0.01 and 0.001. In the remaining elements, $d_e = 0$.

Mesh	1	2	3	4
No. of elements	65	129	193	257

Table 1: Number of elements in each mesh.

Figure 2 shows the damage indicators $CD_{1,w}$ and $CD_{1,M}$ with the corresponding quality evaluators $\mu_{1,w}$ and $\mu_{1,M}$ for the three values of the damage parameter, using mode 1 and 257 elements (Mesh 4). It can be seen that the damage indicator based on displacements has a worse performance when the damage is small, while the damage indicator based on bending moments has a similar behaviour for the three levels of damage. In these cases, the quality evaluators always decrease when the quality of the damage localisation decreases. On the other hand, Figure 3 shows the damage indicators $CD_{4,w}$ and $CD_{4,M}$ with the corresponding quality evaluators $\mu_{4,w}$ and $\mu_{4,M}$ for the three values of the damage parameter, using mode 4 and 129 elements (Mesh 2). In this case, for the damage indicator based on displacements, high values of the quality evaluator do not necessarily correspond to good damage localisations, due to the noise at the ends of the beam. The possibility of higher values of the quality evaluator
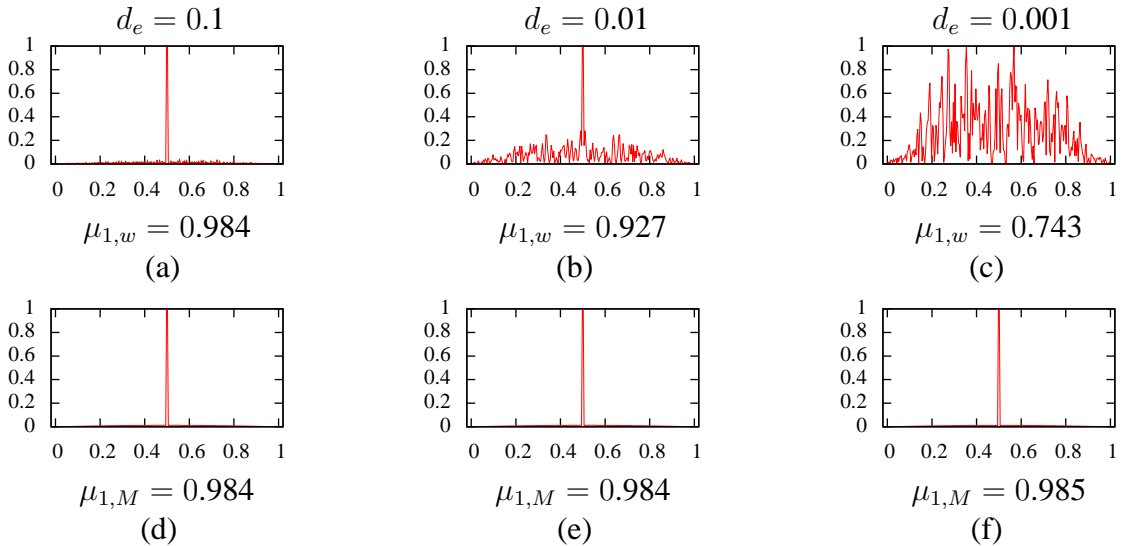

Figure 2: Damage indicators $CD_{1,w}$ ((a)-(c)) and $CD_{1,M}$ ((d)-(f)), with the corresponding $\mu_{1,w}$ and $\mu_{1,M}$ for damage parameters $d_e = 0.1$ ((a) and (d)), $d_e = 0.01$ ((b) and (e)), $d_e = 0.001$ ((c) and (f)), using 257 elements (Mesh 4).
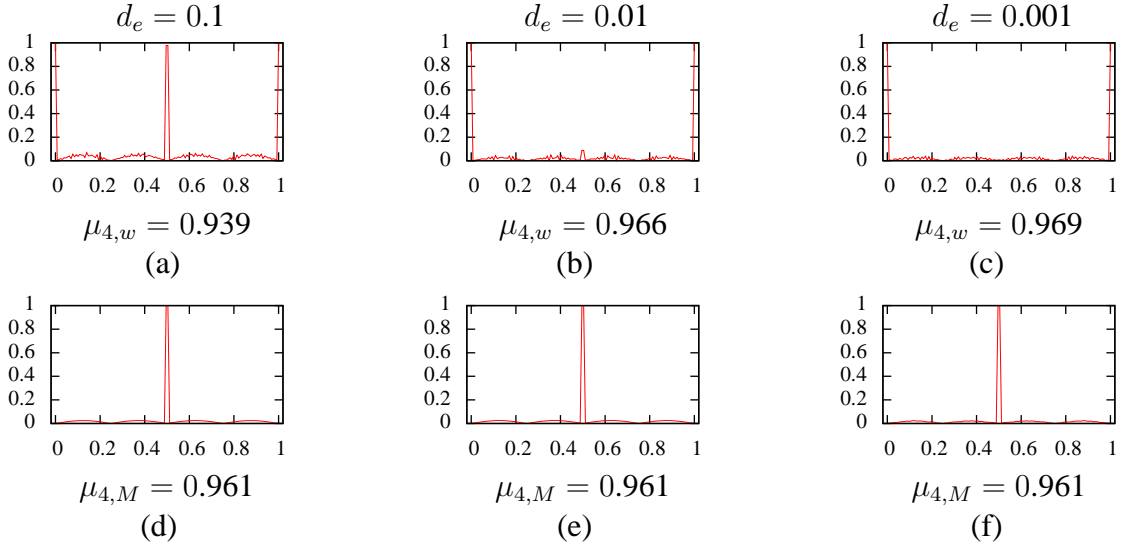
7

Figure 3: Damage indicators $CD_{4,w}$ ((a)-(c)) and $CD_{4,M}$ ((d)-(f)), with the corresponding $\mu_{4,w}$ and $\mu_{4,M}$ for damage parameters $d_e = 0.1$ ((a) and (d)), $d_e = 0.01$ ((b) and (e)), $d_e = 0.001$ ((c) and (f)), using 129 elements (Mesh 2).

corresponding to bad damage localisations has been previously suggested in [15].

Tables 2, 3 and 4 show the quality evaluators $\mu_{q,w}$ and $\mu_{q,M}$ for the three values of the damage parameter, using the first four modes and the meshes described in Table 1. The cases where the higher values of the damage indicators are not near the center, i.e. bad damage localisations, are indicated in bold type. If the bad localisation cases are ignored, the quality evaluators based on displacements decrease when the damage decreases. However, it can be seen that the quality evaluators based on bending moments have small differences when the damage changes. Furthermore, there are no bad damage localisations. This means that this damage indicator is very good to localise the damage.

	$\mu_{q,w}$				$\mu_{q,M}$			
Mesh	$q = 1$	$q = 2$	$q = 3$	$q = 4$	$q = 1$	$q = 2$	$q = 3$	$q = 4$
1	0.939	**0.879**	0.922	**0.925**	0.939	0.939	0.923	0.939
2	0.969	0.934	0.961	**0.939**	0.969	0.969	0.961	0.969
3	0.979	0.838	0.974	0.959	0.979	0.980	0.974	0.979
4	0.984	**0.757**	0.981	0.947	0.984	0.984	0.981	0.984

Table 2: Quality evaluators $\mu_{q,w}$ and $\mu_{q,M}$ when the damage parameter has a value of $d_e = 0.1$ (bold type indicates bad damage localisations).

4 CONCLUSIONS

The use of mixed finite elements for the analysis of beams subjected to damage is presented in this paper. This kind of finite elements allows the direct computation of curvatures and, therefore, there is no need for the application of finite differences to the displacements in order to obtain them. To illustrate the advantages of this approach, a comparison between the quality of the damage localisations based on curvatures obtained using mixed finite elements and conventional finite elements through the use of finite differences is presented. The advantages are even

Mesh	$\mu_{q,w}$				$\mu_{q,M}$			
	$q=1$	$q=2$	$q=3$	$q=4$	$q=1$	$q=2$	$q=3$	$q=4$
1	0.938	**0.934**	0.888	**0.938**	0.939	0.939	0.925	0.939
2	0.967	**0.861**	0.959	**0.966**	0.969	0.969	0.961	0.969
3	0.954	**0.664**	0.974	**0.949**	0.979	0.982	0.974	0.980
4	0.927	**0.814**	0.979	**0.831**	0.984	0.983	0.981	0.982

Table 3: Quality evaluators $\mu_{q,w}$ and $\mu_{q,M}$ when the damage parameter has a value of $d_e = 0.01$ (bold type indicates bad damage localisations).

Mesh	$\mu_{q,w}$				$\mu_{q,M}$			
	$q=1$	$q=2$	$q=3$	$q=4$	$q=1$	$q=2$	$q=3$	$q=4$
1	0.916	**0.939**	**0.933**	**0.939**	0.940	0.936	0.925	0.940
2	0.879	**0.866**	0.932	**0.969**	0.969	0.967	0.961	0.972
3	**0.735**	**0.670**	0.944	**0.946**	0.980	0.975	0.975	0.987
4	**0.743**	**0.764**	0.918	**0.839**	0.985	0.957	0.981	0.958

Table 4: Quality evaluators $\mu_{q,w}$ and $\mu_{q,M}$ when the damage parameter has a value of $d_e = 0.001$ (bold type indicates bad damage localisations).

noticeable if one uses an optimized sampling technique used to reduce the noise propagation when conventional finite elements are used.

ACKNOWLEDGMENTS

REFERENCES

[1] S. W. Doebling, C. R. Farrar, M. B. Prime, and D. W. Shevitz, *Damage identification and health monitoring of structural and mechanical systems from changes in their vibration characteristics: A literature review*. Technical Report LA–13070–MS, Los Alamos National Laboratory, 1996.

[2] J. V. Araújo dos Santos, N. M. M. Maia, C. M. Mota Soares, and C. A. Mota Soares, Structural damage identification: A survey. *Trends in computational structures technology*, Saxe-Coburg Publications, Stirlingshire, UK, 1–24, 2008.

[3] W. Fan and P. Qiao, Vibration-based damage identification methods: A review and comparative study. *Structural Health Monitoring*, **10** (1), 83–111, 2011.

[4] A.K. Pandey, M. Biswas, and M.M. Samman, Damage detection from changes in curvature mode shapes. *Journal of Sound and Vibration*, **145** (2), 321–332, 1991.

[5] E. Sazonov and P. Klinkhachorn, Optimal spatial sampling interval for damage detection by curvature or strain energy mode shapes. *Journal of Sound and Vibration*, **285** (4–5), 783–801, 2005.

[6] M. Chandrashekhar and R. Ganguli, Damage assessment of structures with uncertainty by using mode-shape curvatures and fuzzy logic. *Journal of Sound and Vibration*, **326** (3–5), 939–957, 2009.

[7] A. Tomaszewska, Influence of statistical errors on damage detection based on structural flexibility and mode shape curvature. *Computers & Structures*, **88** (3–4), 154–164, 2010.

[8] M. Radzienski, M. Krawczuk, and M. Palacz, Improvement of damage detection methods based on experimental modal parameters, *Mechanical Systems and Signal Processing*, **25** (6), 2169–2190, 2011.

[9] N. M. M. Maia, J. M. M. Silva, E. A. M. Almas, and R. P. C. Sampaio, Damage detection in structures: From mode shape to frequency response function methods, *Mechanical Systems and Signal Processing*, **17** (3), 489–498, 2003.

[10] N. M. M. Maia, J. V. Araújo dos Santos, R. P. C. Sampaio, and C. M. Mota Soares, Damage identification using curvatures and sensitivities of frequency-response-functions. Alfredo Güemes ed. *Third European Workshop on Structural Health Monitoring*, Granada, Spain, 547–554, 2006.

[11] J. N. Reddy, *Energy principles and variational methods in applied mechanics*. John Wiley, NY, 2nd edition, 2002.

[12] J. Lemaitre, *A Course on Damage Mechanics*. Springer-Verlag, Berlin Heidelberg, 2 edition, 1996.

[13] M. Abramowitz and I. A. Stegun eds, *Handbook of mathematical functions with formulas, graphs, and mathematical tables*. Dover Publications, Inc., New York, 1972.

[14] P. Moreno-García, H. Lopes, J. V. Araújo dos Santos, and N. M. M. Maia, Damage localisation in composite laminated plates using higher order spatial derivatives. B. H. V. Topping ed. *Eleventh International Conference on Computational Structures Technology*, Civil-Comp Press, Dubrovnik, Croatia, Paper 75, 2012.

[15] P. Moreno-García, H. Lopes, J. V. Araújo dos Santos, and N. M M. Maia, Application of higher order derivatives to damage localisation in laminated composite plates. *Computers & Structures*, (submitted).

[16] J. R. Gartner and N. Olgac, Improved numerical computation of uniform beam characteristic values and characteristic functions. *Journal of Sound and Vibration*, **84** (2), 481–489, 1982.

[17] P. Moreno-García, J. V. Araújo dos Santos, and H. Lopes, A new technique to optimize the use of mode shape derivatives to localise damage in laminated composite plates. *17th International Conference on Composite Structures (ICCS17)*, Porto, Portugal, Paper 3485, 2013.